

# Research on The SWIPT System Throughput Based on Interference Signal Energy Collecting

**Jianxiong Li<sup>1</sup>, and Hailong Jiang<sup>2\*</sup>**

<sup>1</sup> School of Electronics and Information Engineering, Tiangong University  
Tianjin, 300387 China  
[e-mail: lijianxiong@tiangong.edu.cn]

<sup>2</sup> School of Electronics and Information Engineering, Tiangong University  
Tianjin, 300387 China  
[e-mail: 250734517@qq.com]

\*Corresponding author: Hailong Jiang

*Received March 23, 2023; revised May 21, 2023; revised June 25, 2023; accepted July 19, 2023;  
published August 31, 2023*

---

## **Abstract**

The general interference is the imperative trouble for simultaneous wireless information and power transfer (SWIPT) system. Although interference has bad influences on the performance of the system, it carries energy simultaneously. In this paper, the energy-constrained relay of the SWIPT system needs to spend much time on energy collecting (EC) in the information transmission (IT) period. Therefore, we propose the scheme of interference signal energy collecting (ISEC) when the interference is strong, and the SWIPT system does not carry out IT. The relay of the system continues to collect energy and stores it until the interference has minimal impact on IT. Then the system performs IT. We divide the collected interference energy equally into several parts, and each IT block receives one part. The proposed scheme is appealing because it can reduce the time of EC in IT period to make the relay spends more time forwarding the received signal in order to improve the performance of the system throughput. Furthermore, we propose a time-switching (TS) protocol based on EC at the relay. And it allows the relay forwarding signal at an appropriate power. Under the protocol, the time of EC can be flexible according to the forwarding power that we give so that the collected energy can be used more efficiently. We give the expressions of the system throughput according to the proposed scheme and protocol. Moreover, the influence of the interference power on the system throughput is also studied.

---

**Keywords:** SWIPT, energy collecting, time-switching, system throughput, general interference

## 1. Introduction

Wireless cooperative networks (WCNs) play a promising role nowadays. Especially for the booming fifth generation (5G) and cloud computing times, it becomes more attractive [1]. However, traditional WCNs are often limited by the general interference and the energy constrained relay node, which inevitably makes a loss of the system throughput. The natural energy sources such as solar energy and water energy are unstable and unsteady, and they are not suitable to provide energy to WCNs. Some researchers had tried to equip the battery to the relay. Though the battery equipped could be displaced, it could devote to high operating costs, inconvenience and even insecurity [2]. Moreover, for the future 6G times, super high density micro cellular network inevitably devotes to the general interference when they are working at ultra-high rate [3]. This unavoidably leads to the poor performance of WCNs. Though a lot of studies had been carried out in [4], the accomplishments were not nearly enough.

In recent years, radio frequency (RF) signal energy harvesting is supposed to a promising method to prolong the lifetime of energy limited wireless networks [5-7]. A distinctive advantage of RF signal energy collecting is that RF signals also carry energy while transmitting information. Radio frequency energy collection (RFEC) techniques can be composed of two categories, including wireless power transfer (WPT) and simultaneous wireless information and power transfer (SWIPT). Traditionally, there are two ways to supply energy to an energy constrained relay node in WCNs. One is to transfer wireless power to the relay node using an electromagnetic device [8], the other is to power the relay by beamforming [9]. The authors in [9] studied the beneficial combination of SWIPT and RF communications in WCNs. SWIPT had raised a growing amount of attention [10]. A significant application of SWIPT is cooperative relay, where the energy limited relay forwards the source signal to the destination. Therefore, energy collection (EC) in the kind of wireless cooperative communication system is vital. In recent years, EC from RF signals in wireless relaying networks was studied in [11-14]. Under the condition of limited EC, considering amplify-forward (AF) relay, the authors in [11] studied the performance of outage in half-duplex relay network and the performance of throughput in full-duplex relay network. In [12], the authors studied the outage performance for the SWIPT energy harvesting (EH) relay system, where the relay was in co-channel interference (CCI), using power splitting (PS) protocol. An AF multiple relay system using SWIPT receivers subjected to interference channels was discussed in [13]. To maximize achievable system rate, the authors proposed a power allocation problem under forwarding power and energy collection limitation. The authors in [14] investigated the SWIPT precoding scheme for K-user multiple-input-multiple-output (MIMO) interference channels (IC).

However, it was practically not feasible to directly decode the carried information from RF signals that were used to harvest energy simultaneously. This inspired the design of practical achievable receiver equipment, which used time-switching (TS) or PS to decode information in the energy collection processes [15-18]. Using a double-hop EC cooperative communication system, the authors in [15] presented the new relay protocols by adaptive-TS for AF and decode-forward (DF) relay modes, respectively. A low complexity resource splitting algorithm for DF relay strategy was proposed in [16], but the algorithm had not taken energy collecting from the interference into account. Moreover, most existing works based on PS focused on the transceiver designs under fading channels. The authors in [17] studied an MIMO orthogonal frequency division multiplexing (OFDM) SWIPT system based in PS strategy, and designed PS ratio to maximize the secrecy rate.

In this paper, we use the AF relay single-input-single-output (SISO) SWIPT system, where a source node transmits signal to the destination by an energy-constrained relay. To improve the performance of the system throughput, an interference signal energy collecting (ISEC) scheme and a TS protocol are proposed.

They are valuable because they can effectively improve the system throughput under the general interference. We give the theoretical mathematical expressions of the system throughput. The provided expressions allow accurate determination of the system throughput based on the system parameters by simulations. The simulation results show that the proposed scheme and protocol are superior to the existing method without using IREC scheme and the TS protocol, and they achieve efficient use of energy by reasonable distribution of the duration of EC.

## 2. Related Work

Recently, there was a novel method to handle the problem, which meant the energy-limited cooperative communication system relay collected the interference signal energy and used it to transmit signal to compensate for the bad effects of interference [18]. So, many scholars had done some research on the matter of interference processing (IP) [19-20], efficient resource allocation strategy [21-24], and energy efficiency (EE) [25-29].

In [19], the authors provided a high-level outline using several different interference processes. The authors in [20] studied two aspects of how to handle interference when channel state information (CSI) was unclear. Excellent resource allocation strategy played an important role in the applications existed in SWIPT system. In [21] a novel method of wireless-powered (WP) MIMO non-orthogonal multiple access (NOMA) was studied by using collecting and forwarding protocol with TS and power control (PC) strategies to get the optimal performance and lifetime. To get more the collected energy and minimize the number of energy subcarriers, the authors in [22] used the time-division multiple access (TDMA) method in multiple EC nodes by the cooperative WPT. The authors in [23] discussed the resource allocation problem for multiple input single output (MISO) NOMA employing SWIPT. In [24], the time resource assignment was discussed in a RF-powered network with the known statistical information about the collected power.

In [25], the authors studied the optimal energy efficiency in wireless device-to-device (D2D) cellular networks in which D2D couples used SWIPT technology. The EE optimization was studied with imperfect CSI in a SWIPT two-tier heterogeneous network in [26]. To get the optimal energy efficiency while using the minimum needed collected energy at each node, the authors in [27] studied the maximal energy efficiency by power distribution at the base station and PS at each node. In [28], the authors used a constant-linear-constant (CLC) EC model, and the throughput and energy EE of the system were optimized by adjusting the TS parameter. However, the EE will reduce when the communication distance is too long, because there is a loss in the spreading process of RF signals. The authors in [29] studied the problem of intelligent reflecting surface (IRS) optimization to improve the EE in a MIMO OFDM SWIPT system with EC model.

## 3. System Model and Assumptions

### 3.1 System Model

We propose a wireless cooperative communication system model that includes a source,

expressed by S, a relay, R and a destination, D. The source and destination are mounted with an antenna, while the relay has double antennas. The antennas at the relay are symmetrical which serve as receiving antenna and forwarding antenna. The source and destination are active and have no energy limitation, whereas the relay node is energy limited. Therefore, the relay needs to collect energy from external environment to maintain its operation. We suppose that there is no direct link between the source to the destination in order to simulate the real-world communication circumstances with physical obstacles. The working strategy of the relay is AF, as shown in Fig. 1.

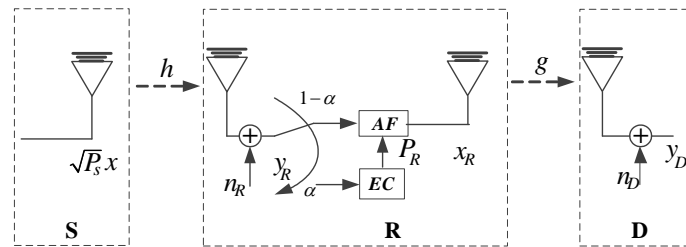


Fig. 1. AF-based SWIPT relay system model

As shown in Fig. 1,  $P_s$  is the transmitting power that the RF signal,  $x$  is the signal from the source and  $E[|x|^2]=1$ , where  $E[\cdot]$  and  $|\cdot|$  are the expectation arithmetic and the absolute arithmetic. The channel fading factor from source-to-relay is  $h$ ,  $y_R$  is the signal picked up in the relay, and  $n_R$  is the additive white Gaussian noise (AWGN) introduced by the receiving antenna at the relay. The relay forwarding power is  $P_R$ , and the amplified signal is  $x_R$ . The channel gain from relay-to-destination is  $g$ , the signal  $x_R$  reaches the destination and  $y_D$  is the received signal. Meanwhile,  $n_D$  is the AWGN introduced by the receiving antenna at the destination. The distances from source-to-relay and from relay-to-destination are  $D_1$  and  $D_2$ .

### 3.2 The assumptions of relay model and channel model

For ease of analysis, we make the following assumptions.

- There are two circuits in the relay carrying out EC and signal forwarding (SF) respectively, and part of time is used for EC and the rest for SF. For we proposed protocol, the time of EC is changeable according to the given forwarding power.
- Compared with the relay-to-destination signal forwarding power, the working power needed by the circuit at the relay can be ignored. The assumption is reasonable in the actual systems when the systems work over very long transmission distances, because the forwarding energy is the main part of energy consumption.
- The duration of the general interference is  $mT$ , which happens before the IT. The average power of the relay collecting energy from the interference signal is  $P_I$ . The duration of IT in the SWIPT system is  $nT$ , every IT block lasting for  $T$ , and  $m, n$  are positive integers. Every IT block is composed of EC and SF, and the duration of EC is  $\alpha T$ , and the rest time is divided into two equal parts used for  $S \rightarrow R$  SF and  $R \rightarrow D$  SF, respectively.  $\alpha$  is the fraction of time that the relay collects energy from the source signal during the IT period without our proposed TS protocol. Strict time synchronization is maintained during IT. The energy collected from the interference is equally distributed

among  $n$  IT blocks. We define  $\beta = m/n$  is the interference ratio. The energy distribution model is shown in Fig. 2.

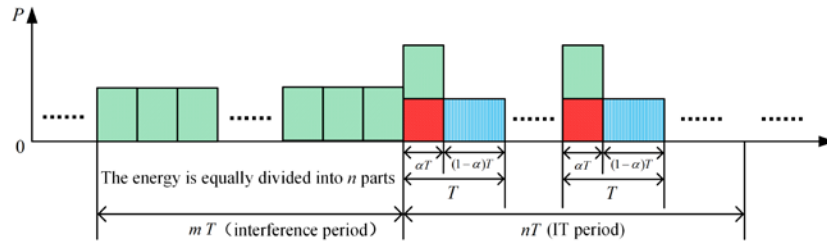


Fig. 2. The energy distribution model

- The channel fading factors,  $h$  and  $g$  are also presumed to be invariable in a block time of  $T$ . We also suppose that  $h$  and  $g$  are independent and identical distributions at every block, subjecting to exponential distribution with mathematical exception of  $\lambda_h$  and  $\lambda_g$ , respectively. The expression is given by

$$f_h(x) = \begin{cases} \frac{1}{\lambda_h} e^{-\frac{x}{\lambda_h}}, & x > 0 \\ 0, & \text{else} \end{cases} \quad (1)$$

$$f_g(y) = \begin{cases} \frac{1}{\lambda_g} e^{-\frac{y}{\lambda_g}}, & y > 0 \\ 0, & \text{else} \end{cases} \quad (2)$$

### 3.3 The working mode of the relay

We consider that the IT time of every block is  $T$ . Generally, every block could perform EC and SF. In order to analyze the process flexibility, we suppose that the energy saving device in the relay has unlimited capacity. When the TS protocol that we proposed is not being applied, which means that the duration of EC in each IT block is equal and fixed.  $\alpha_k$  is the fraction of time that the relay collects energy from the source signal in the  $k$ -th block during the IT period without our proposed TS protocol. The working mode one in the relay is shown in Fig. 3.

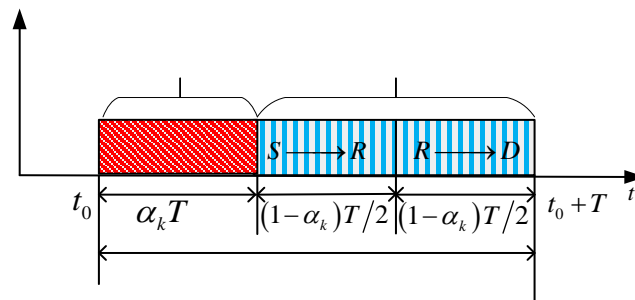


Fig. 3. Illustration of EH and IT blocks

Just described in Fig. 3, at the start of every block, the relay performs EC. During EC, the relay collects energy from the RF signal. During SF, the total energy from the RF signal and the interference is utilized to forward the received signal. While under our given protocol, the duration of EC in each IT block,  $\alpha'_k$ , is flexible and it is related to the given AF power.  $\alpha'_k$  is the fraction of time that the relay collects energy from the source signal in the  $k$ -th block during the IT period with our proposed TS protocol. The working mode two in the relay is shown in Fig. 4.

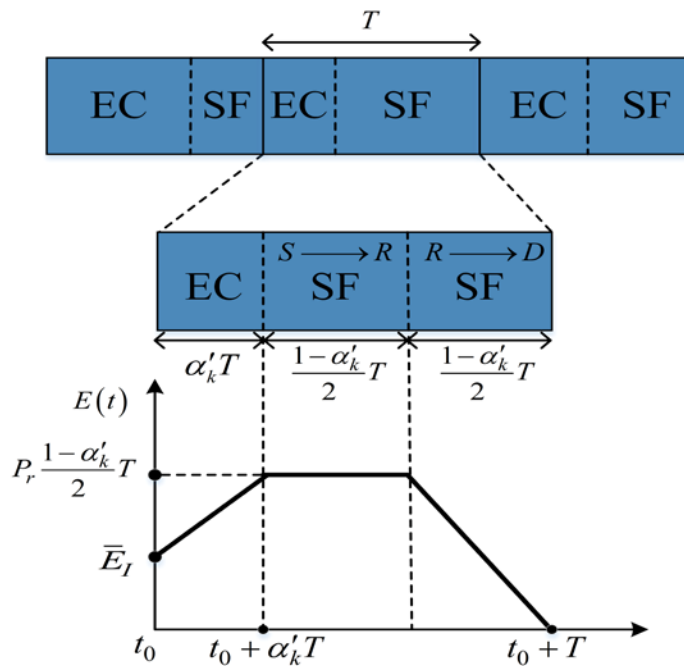


Fig. 4. Illustration of working mode two in the relay

In this situation, the relay sustains to collect energy from the RF signal on the basis of  $\bar{E}_I$  until the total energy is equal to the needed energy that the relay forwards the signal from the source to the destination at an appropriate AF power,  $P_r$ , in the time of  $(1-\alpha')T/2$ .  $P_r$  is the given AF power according the proposed TS protocol.  $\bar{E}_I$  is the total energy that is distributed to each IT block. So,  $\alpha'_k$  is subject to the AF power we set. In practical situations,  $\bar{E}_I$  is not very big, so we assume that  $\alpha'_k \geq 0$ . That means the relay always need to collect extra energy from the received RF signal. In this working model, the energy efficiency is higher than working mode one. In this paper, in order to be operated easily, we suppose that the relay can gets channel status information.

In the following sections, we use the system throughput as the evaluation criterion. It means that the part of the block time used for SF in the whole duration of IT.

#### 4. Proposed protocol and scheme

In this section, we calculate the expressions of the signal model and the collected energy firstly, and then using the relevant expressions to compute the system throughput based on the proposed scheme and protocol.

#### 4.1 Energy Collection

According to the assumptions made above, in the strong interference existing period, the expression of energy collected from the interference signal,  $E_I$ , can be given as

$$E_I = \eta P_I m T \quad (3)$$

where  $0 < \eta < 1$  is the energy harvesting efficiency.

The energy that can be distributed to each IT block,  $\bar{E}_I$ , is

$$\bar{E}_I = \frac{E_I}{n} = \frac{\eta P_I m T}{n} = \eta \beta P_I T \quad (4)$$

When the strong interference ends, the system performs IT. The relay forwards the RF signal received from the source to the destination. For the  $k$ -th block, without TS protocol, the expression of energy collected from the RF signal,  $E_{RF}$ , can be expressed as

$$E_{RF} = \frac{\eta P_S h_k}{D_1^m} \alpha_k T \quad (5)$$

where  $k$  is the block indicator,  $m$  is the path loss coefficient.

When the Time Switching protocol that we proposed is not being applied, the AF power of the  $k$ -th IT block,  $P_R$ , is expressed as

$$P_R = \frac{E_{RF} + \bar{E}_I}{(1 - \alpha_k)T/2} = \frac{2\eta(\beta P_I D_1^m + \alpha_k P_S h_k)}{D_1^m (1 - \alpha_k)} \quad (6)$$

where  $\alpha_k$  is the duration of EC in the IT block.

While under our given protocol,  $\alpha'_k$ , is flexible and it is related to the given AF power. We define the forwarding power that we give is  $P_r$ , then the needed energy to forward the source signal to the destination during the time of  $(1 - \alpha')T/2$ ,  $E_{SF}$ , can be expressed as

$$E_{SF} = P_r \frac{(1 - \alpha'_k)T}{2} \quad (7)$$

In this situation, the energy collected from the RF signal,  $E'_{RF}$ , is

$$E'_{RF} = \frac{\eta P_S h'_k}{D_1^m} \alpha'_k T \quad (8)$$

Through (4), (7) and (8), that  $E_{SF} = E'_{RF} + \bar{E}_I$ , the flexible value of duration of EC,  $\alpha'_k$ , can be expressed as

$$\alpha'_k = \frac{P_r D_1^m - 2\eta \beta D_1^m P_I}{2\eta P_S h'_k + P_r D_1^m} \quad (9)$$

We can see that the numerator of (9) is smaller than  $P_r D_1^m$ , and  $P_r D_1^m$  is smaller than the denominator of (9). This means the value of  $\alpha'_k$  is always between 0 and 1. This shows that our proposed protocol is reasonable because we assume that the energy saving device in the relay has unlimited capacity. We can set an appropriate AF power value depending on the actual IT situation to achieve maximum throughput of the system. The performance of the

system throughput in each block is different because it is related to  $\alpha'_k$ , which is subject to the channel fading factor,  $h$ . The system throughput in this paper means the part that performs SF in the whole IT block time in non-interruption status.

## 4.2 Throughput Analysis

### 4.2.1 Throughput Analysis Without Using Proposed Protocol

When the system carries out IT, the expression of the RF signal received from the source in the  $k$ -th block can be given as

$$y_R = \sqrt{\frac{P_S}{D_1^m}} h_k x_k + n_R \quad (10)$$

After amplification and forwarding, the signal  $x_R$  transmitted by the relay is.

$$x_R = \mu y_R = \sqrt{\frac{P_R D_1^m}{P_S h_k + \sigma_R^2 D_1^m}} y_R \quad (11)$$

where  $\mu = \sqrt{\frac{P_R}{(P_S h_k / D_1^m) + \sigma_R^2}}$  is the magnification of AF relay, and  $\sigma_R^2$  is the variance of  $n_R$ .

During IT period, the signal received in the destination is

$$y_D = \frac{1}{\sqrt{D_2^m}} g_k x_R + n_D \quad (12)$$

Substituting (11) into (12),  $y_D$  can be rewritten as

$$y_D = \sqrt{\frac{P_R P_S h_k g_k}{D_2^m (P_S h_k + \sigma_R^2 D_1^m)}} x_k + \sqrt{\frac{P_R D_1^m g_k}{D_2^m (P_S h_k + \sigma_R^2 D_1^m)}} n_R + n_D \quad (13)$$

Using (13), without TS protocol, the Signal to Noise Ratio (SNR) at the destination,  $\gamma_D$  can be summarized as

$$\gamma_D = \frac{\frac{P_R P_S h_k g_k}{D_2^m (P_S h_k + \sigma_R^2 D_1^m)}}{\frac{P_R D_1^m g_k \sigma_R^2}{D_2^m (P_S h_k + \sigma_R^2 D_1^m)} + \sigma_D^2} = \frac{P_R P_S h_k g_k}{P_R D_1^m g_k \sigma_R^2 + \sigma_D^2 D_2^m (P_S h_k + \sigma_R^2 D_1^m)} \quad (14)$$

where  $\sigma_D^2$  is the variance of  $n_D$ .

If the SNR of the system,  $\gamma_D$ , is less than the SNR threshold  $\gamma_0$ , the  $k$ -th block during IT period will be in interruption status. So, without TS protocol, the interruption probability of the system in the  $k$ -th block,  $pout_k$  can be expressed as

$$pout_k = p(\gamma_D < \gamma_0) \quad (15)$$

Substituting (14) into (15),  $pout_k$  can be rewritten as



$$pout_k = p\left(\left(a_k |h_k|^2 - b_k h_k - c_k\right) g_k < d_k h_k + e_k\right) \quad (16)$$

The constants that are relative the system parameters to calculate  $pout_k$  conveniently without TS protocol can be described as follows

$$\begin{cases} a_k = 2\eta\alpha_k P_S^2 \\ b_k = 2\eta\alpha_k D_1^m P_S^2 \sigma_R^2 \gamma_0 - 2\eta\beta P_S P_I D_1^m \\ c_k = 2\eta\beta P_I \sigma_R^2 D_1^{2m} \gamma_0 \\ d_k = D_1^m D_2^m \sigma_D^2 (1 - \alpha_k) P_S \gamma_0 \\ e_k = D_1^{2m} D_2^m \sigma_D^2 \sigma_R^2 (1 - \alpha_k) \gamma_0 \\ \Delta_k = a_k |h_k|^2 - b_k h_k - c_k \end{cases} \quad (17)$$

According to (17),  $pout_k$  can be specifically expressed as

$$pout_k = \begin{cases} p\left(g_k < \frac{d_k h_k + e_k}{a_k |h_k|^2 - b_k h_k - c_k}\right) & \Delta_k > 0 \\ p\left(g_k > \frac{d_k h_k + e_k}{a_k |h_k|^2 - b_k h_k - c_k}\right) = 1 & \Delta_k < 0 \end{cases} \quad (18)$$

Substituting (1) and (2) into (18), the integral expression of the interruption probability is

$$\begin{aligned} pout_k &= \int_0^{h_1} f_h(x) \cdot p\left(g > \frac{d_k h_k + e_k}{a_k |h_k|^2 - b_k h_k - c_k}\right) dx \\ &+ \int_{h_1}^{\infty} f_h(x) \cdot p\left(g < \frac{d_k h_k + e_k}{a_k |h_k|^2 - b_k h_k - c_k}\right) dx \\ &= \int_0^{h_1} f_h(x) dx + \int_{h_1}^{\infty} f_h(x) \cdot \left(1 - e^{-\frac{d_k x + e_k}{\lambda_g (a_k x^2 - b_k x - c_k)}}\right) dx \end{aligned} \quad (19)$$

$$\text{where } h_1 = \frac{b_k + \sqrt{b_k^2 + 4a_k c_k}}{2a_k}$$

According to the definition of the throughput, without TS protocol, the system throughput in the  $k$ -th block,  $\tau_k$ , can be expressed as

$$\tau_k = (1 - pout_k) \frac{(1 - \alpha_k) T}{T} = (1 - \alpha_k) (1 - pout_k) \quad (20)$$

#### 4.2.2 Throughput Analysis Using Proposed Protocol

The IT process is similar with that in subsection 4.2.1. But in this subsection, according to the protocol we proposed,  $P_r$  can be seen as a constant. The SNR of the system in the  $k$ -th,  $\gamma'_D$  can be expressed as

$$\gamma'_D = \frac{\frac{P_r P_S h'_k g'_k}{D_2^m (P_S h'_k + \sigma_R^2 D_1^m)}}{\frac{P_r D_1^m g'_k \sigma_R^2}{D_2^m (P_S h'_k + \sigma_R^2 D_1^m)} + \sigma_D^2} = \frac{P_r P_S h'_k g'_k}{P_r D_1^m g'_k \sigma_R^2 + \sigma_D^2 D_2^m (P_S h'_k + \sigma_R^2 D_1^m)} \quad (21)$$

According to (15), with TS protocol, the interruption probability in this subsection,  $pout'_k$  is

$$pout'_k = p((a'_k h'_k - b'_k) g'_k < c'_k h'_k + d'_k) \tag{22}$$

The constants that are relative the system parameters to calculate  $pout'_k$  conveniently with TS protocol can be described as follows

$$\begin{cases} a'_k = P_S P_r \\ b'_k = P_r D_1^m \sigma_R^2 \gamma_0 \\ c'_k = P_S D_2^m \sigma_D^2 \gamma_0 \\ d'_k = D_1^m D_2^m \sigma_R^2 \sigma_D^2 \gamma_0 \end{cases} \tag{23}$$

According (23),  $pout'_k$  can be specifically expressed as

$$\begin{aligned} pout'_k &= p((a'_k h'_k - b'_k) g'_k < c'_k h'_k + d'_k) \\ &= \begin{cases} p\left(g'_k < \frac{c'_k h'_k + d'_k}{a'_k h'_k - b'_k}\right) & h'_k > \frac{b'_k}{a'_k} \\ p\left(g'_k > \frac{c'_k h'_k + d'_k}{a'_k h'_k - b'_k}\right) = 1 & h'_k < \frac{b'_k}{a'_k} \end{cases} \end{aligned} \tag{24}$$

Substituting (1) and (2) into (24), the integral expression of the interruption probability  $pout'_k$  is

$$\begin{aligned} pout'_k &= \int_0^{\frac{b'_k}{a'_k}} f_h(x) \cdot p\left(g'_k > \frac{c'_k h'_k + d'_k}{a'_k h'_k - b'_k}\right) dx \\ &\quad + \int_{\frac{b'_k}{a'_k}}^{\infty} f_h(x) \cdot p\left(g'_k < \frac{c'_k h'_k + d'_k}{a'_k h'_k - b'_k}\right) dx \\ &= \int_0^{\frac{b'_k}{a'_k}} f_h(x) dx + \int_{\frac{b'_k}{a'_k}}^{\infty} f_h(x) \cdot \left(1 - e^{-\frac{c'_k x + d'_k}{\lambda_g (a'_k x - b'_k)}}\right) dx \end{aligned} \tag{25}$$

According to the definition of the throughput, with TS protocol, the system throughput in the  $k$ -th block in this subsection,  $\tau'_k$ , can be expressed as

$$\tau'_k = E_{h'_k, g'_k} \left\{ (1 - pout'_k) (1 - \alpha'_k) \right\} \tag{26}$$

Since the  $\alpha'_k$  is unrelated to  $g'_k$ , the above equation can be rewritten as

$$\tau'_k = E_{h'_k} \left\{ E_{g'_k} \left\{ 1 - pout'_k \right\} (1 - \alpha'_k) \right\} \tag{27}$$

Substituting (9) and (25) into (27), we can get

$$\begin{aligned}\tau'_k &= \int_{\frac{b'_k}{a'_k}}^{+\infty} \frac{1 - \alpha'_k}{2} (1 - p_{out'_k}) \\ &= \int_{\frac{b'_k}{a'_k}}^{+\infty} \frac{e^{-\left(x + \frac{c'_k x + d'_k}{a'_k x - b'_k}\right)}}{2} dx - \frac{D_1^m P_r - 2\eta\beta D_1^m P_I}{2} \int_{\frac{b'_k}{a'_k}}^{+\infty} \frac{e^{-\left(x + \frac{c'_k x + d'_k}{a'_k x - b'_k}\right)}}{2\eta P_S x + D_1^m P_r} dx\end{aligned}\quad (28)$$

To facilitate the calculation, we define a new variable  $\bar{x} = x - \frac{b'_k}{a'_k}$ , and the above equation can be rewritten as

$$\begin{aligned}\tau'_k &= \frac{e^{-\frac{b'_k + c'_k}{a'_k}}}{2} \int_0^{+\infty} e^{-\frac{\bar{x} - \frac{a'_k d'_k + b'_k c'_k}{(a'_k)^2 \bar{x}}}{(a'_k)^2 \bar{x}}} d\bar{x} \\ &\quad - \frac{e^{-\frac{b'_k + c'_k}{a'_k}}}{2} (D_1^m P_r - 2\eta\beta D_1^m P_r) \int_0^{+\infty} \frac{e^{-\frac{\bar{x} - \frac{a'_k d'_k + b'_k c'_k}{(a'_k)^2 \bar{x}}}{(a'_k)^2 \bar{x}}}}{2a'_k \eta P_S \bar{x} + 2\eta P_S b'_k + a'_k D_1^m P_r} d\bar{x} \\ &= \frac{e^{-\frac{b'_k + c'_k}{a'_k}}}{2} (u K_1(u) - (D_1^m P_r - 2\eta\beta D_1^m P_r) \phi)\end{aligned}\quad (29)$$

where  $u$  and  $\phi$  are defined as

$$\begin{cases} u \triangleq \sqrt{\frac{4(a'_k d'_k + b'_k c'_k)}{(a'_k)^2}} \\ \phi \triangleq \int_{x=0}^{+\infty} \frac{e^{-\frac{x - \frac{a'_k d'_k + b'_k c'_k}{(a'_k)^2 \bar{x}}}{(a'_k)^2 \bar{x}}}}{2a'_k \eta P_S \bar{x} + 2\eta P_S b'_k + a'_k D_1^m P_r} d\bar{x} \end{cases}\quad (30)$$

where  $\int_0^{\infty} e^{-\frac{\beta}{4x} - \gamma x} dx = \sqrt{\frac{\beta}{\gamma}} K_1(\sqrt{\beta\gamma})$ .

## 5. Simulations and analysis

In this section, we give numerical results to prove the performance of the proposed protocol and scheme. The throughput can be analyzed as a function of the system parameters. We adopt the actual simulation parameter values recommended in recent research papers on SWIPT. We set the source transmission power,  $P_S = 10$ , and the path loss coefficient,  $m = 2.7$ .  $\lambda_h = \lambda_g = 1$  is also set. The average power of the relay collecting energy from the interference signal is  $P_I = 5$ , and for convenience of analysis, we set the distance,  $D_1 = D_2 = 1$ . We set the energy collecting efficiency  $\eta = 0.5$ . If there are no special instructions given, we set the threshold SNR,  $\gamma_0 = 1$ , the interference ratio  $\beta = 0.1$  and the noise variances at the relay and the destination nodes,  $\sigma_R^2 = 0.1$ , and  $\sigma_D^2 = 0.1$ , respectively.

### 5.1 Simulation Without the Proposed TS Protocol

In this subsection, we give simulation results to verify the analytical results without using the proposed TS protocol, and make comparison with an AF relaying wireless network under EC limitations in [30-31]. The proposed method in [30] did not allow relay to collect energy from interference, and EC time-duration accounted for a fixed proportion of the whole IT time. Another method being discussed in [31] took energy collection into consideration, and the authors studied the effect of interference energy harvesting (IEH) on the relay system rate. According to the proposed IEH scheme in [31], we calculate the corresponding system throughput using the same system parameters. In the simulations, we calculate the throughput  $\tau$  of about  $n=1000$  IT blocks in the same way according to the independent  $h$  and  $g$  in each IT block and the average of the total throughput was used as our final assessment criteria.

Without our proposed TS Protocol, Fig. 5 describes the system throughput,  $\tau$ , versus the duration of EC,  $\alpha$ , with the ISEC scheme in this paper, without ISEC in [30], and with the IEH scheme in [31], respectively. As shown in Fig. 5, we can know that the system throughput increases firstly and then reduces with increasing of the fixed TS coefficient  $\alpha$ . This is because when the value of  $\alpha$  is less than 0.27, 0.28 or 0.36, the energy collected from the received signal increases which devotes to the increase of  $P_R$  with the increase of  $\alpha$ . And the system outage probability reduces with the increase of  $P_R$ . Though the SF time-duration also reduces a little, but it is not the main factor that influences the system throughput. However, if the value of  $\alpha$  is more than 0.27, 0.28 or 0.35 and continuously increases, the duration of EC accounts for a large proportion of each IT block, which devotes the duration of SF becomes smaller and smaller. We can also see that the throughput performance is not obviously better than the proposed method mentioned in [31]. There are two main reasons for this. The first reason is that the simulation results in Fig. 5 are provided under the circumstance that our proposed protocol is not adopted. The second reason is that we calculate the corresponding system throughput according to the given equations in [31]. The authors in [31] did not consider signal fading during the signal transmission. However, the throughput in our paper is still slightly higher than the throughput in [31]. This proves the viability of our proposed scheme.

The proposed scheme has a better performance, but the gap is gradually narrowing when  $\alpha$  is close to 1. This better performance of the proposed scheme is due to more efficient use of interference sources. If the relay works with the fixed time-duration EC, without collecting energy from the interference, the collected energy only from RF signal in each block is not controllable and relates to the channel quality of the  $S \rightarrow R$  link. If the  $S \rightarrow R$  link is in deep fade, the only energy collected from the signal will be very small which will decrease the AF power and then results in outage at the destination. When the  $S \rightarrow R$  link is very strong, the collected energy will be very large, which guarantees a large relay AF power but causes a waste of energy. On the other hand, the narrowing gap is because the energy collected from interference can be ignored compared with the energy collected from RF signal when  $\alpha$  is close to 1.

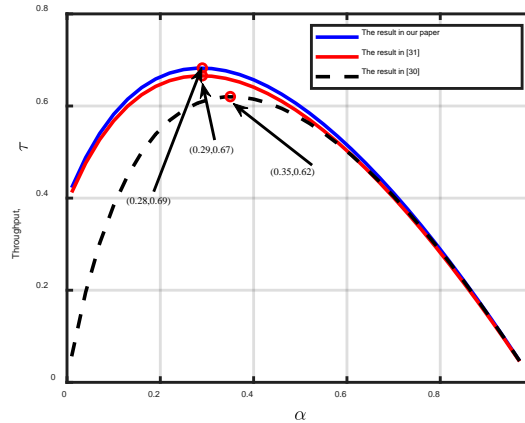


**Fig. 5.** Throughput with respect to the duration of EC

We define  $\alpha^*$  is the value of  $\alpha$  when the system throughput gets its maximum. **Fig. 6** is the relation among the optimum system throughput, the optimum EC duration  $\alpha^*$  and the average power of the relay collecting energy from the interference,  $P_I$ . In **Fig. 6**, the optimum system throughput and the optimum remain unchanged with the addition of  $P_I$  without ISEC scheme. Because there is no interference energy collected in this situation. However, the optimum system throughput is increasing with the increase of  $P_I$ , and the optimum EC duration reduces with ISEC. This is because the large value of  $P_I$  is equivalent to shortening the time that takes for the relay to collect energy from the RF signal. Then the SF duration time takes a large part in the whole IT block time and the AF power is also increasing. These devote to an increasing in system throughput.

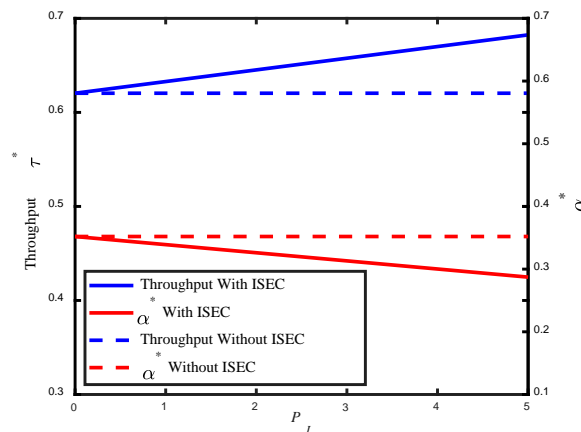


**Fig. 6.** Throughput and EC duration with respect to  $P_I$

The relation among the optimum system throughput, the optimum EC duration  $\alpha^*$  and the interference ratio  $\beta$  is described in **Fig. 7**, where  $0 < \beta < 1$ . In **Fig. 7**, the optimum system throughput decreases with the increase of  $\beta$ , and it decreases more slowly when using ISEC scheme. The optimum EC duration  $\alpha^*$  reduces rapidly and remain unchanged when ISEC is

used or not. With the increase of  $\beta$ , the duration of the interference makes up a large proportion of the total communication time, which shortens the IT time used to forward the signal and causes the decrease of the system throughput. In contrast, with the ISEC scheme, the higher interference energy collected by the relay, the higher the AF power provided for the signal, and the interference energy collected by the relay is moderating the bad impact of the reduced IT time. The unchanged optimum EC duration is because the IT block is not allocating interference energy. We can also get that when  $\beta$  is larger than 0.65,  $\alpha^*$  becomes 0. That means the relay no longer collects energy from the RF signal and performs SF only with the energy collected from the interference signal.

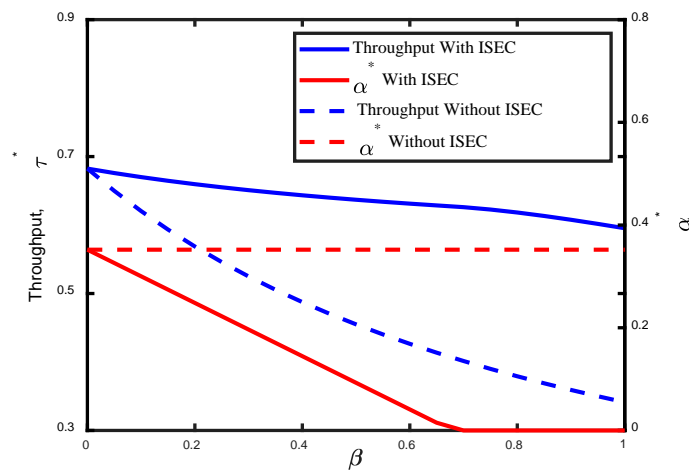


Fig. 7. Throughput and EC duration with respect to  $\beta$

## 5.2 Simulation With the Proposed TS Protocol

Fig. 8 depicts the relation among the system throughput, the flexible EC duration  $\alpha'$  and the given AF power  $P_r$  with the proposed TS protocol. We discover that the system throughput increases firstly and then reduces when  $P_r$  increases, and the EC duration  $\alpha'$  increases sustainably. It is easy to understand. In every IT block, the channel fading factor can be considered unchanging. So, the value of  $\alpha'$  is subject to  $P_r$ . The higher the AF power we provide, the higher RF signal energy collected by the relay. As  $P_r$  increases from 0 to 3, the probability of system interruption decreases. Though the duration of SF is also smaller, but at this situation, it is not the main factor that influences the system throughput. When  $P_r$  is larger than 3 and continues to increase, the increase in AF power cannot compensate for the decrease in SF time. In this situation, the duration of SF is the main factor. According to Fig. 8, we can set  $P_r = 3$ , and at this moment  $\alpha'$  is 0.4. We can determine that the system throughput increases by about 6.3% through making comparison with that in Fig. 5.

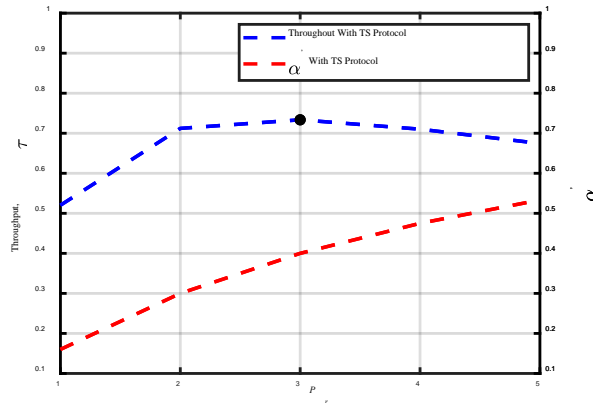


Fig. 8. Optimal throughput with respect to  $P_r$

### 5.3 Comparison With or Without the Proposed TS Protocol

The system throughput as a function of  $P_l$  is given in Fig. 9. In this situation, ISEC is taking and we make  $\alpha = 0.28$  without TS protocol and  $P_r = 3$  with this TS protocol. The system throughput increases with increasing of  $P_l$ , and the protocol we give has a better performance. The reason is similar with that in Fig. 6.

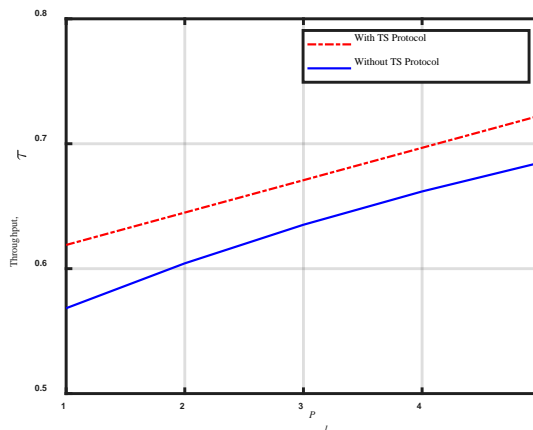
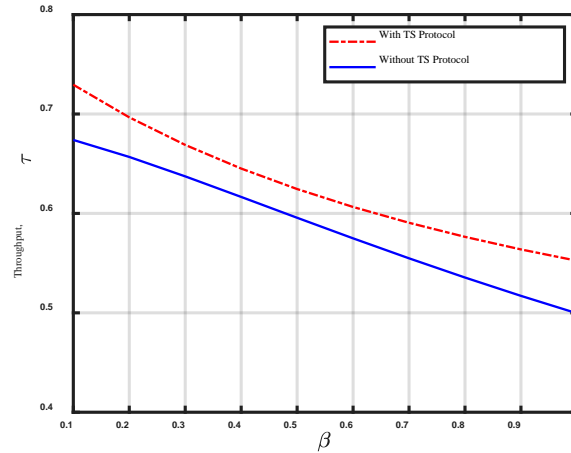


Fig. 9. The system throughput with respect to  $P_l$

Fig. 10 plots the relation between the system throughput and the interference ratio  $\beta$ . In this situation, ISEC is taking and we make  $\alpha = 0.28$  without TS protocol and  $P_r = 3$  with this protocol. We can summarize from Fig. 10 that the system throughput reduces with the addition of  $\beta$ , and it reduces slowly with our protocol. It is easy to understand. The increase of  $\beta$  shortens the IT time used to SF devoting to the decrease of the system throughput.



**Fig. 10.** The system throughput with respect to  $\beta$

## 6. Conclusions

In this paper, an ISEC scheme and a TS protocol are proposed to reduce the loss of system throughput. The scheme and protocol are proved workable, and the approximative optimal fraction of time that the relay collects energy from the source signal during the information transmission (IT) is got. Next, the optimal forwarding power is got according to the proposed the protocol. The expressions of the system throughput are derived. The numerical simulation results show that the ISEC scheme with the TS protocol can effectively improve the system throughput. In addition, this paper investigates the influence of the interference power and interference ratio on the system throughput. The results show that using the protocol has better performance in the different interference power and interference ratio than without the protocol.

## Acknowledgement

This work was supported by the National Natural Science Foundation of China (Grant No. 61372011)

## References

- [1] Z. Wang, T. Li, and L. Ge, et al., "Learn from Optimal Energy-Efficiency Beamforming for SWIPT-Enabled Sensor Cloud System Based on DNN," *IEEE Access*, vol. 9, pp. 60841-60852, Apr. 2021. [Article \(CrossRef Link\)](#)
- [2] R. Zhang and C. K. Ho, "MIMO Broadcasting for Simultaneous Wireless Information and Power Transfer," in *Proc. of 2011 IEEE Global Telecommunications Conference - GLOBECOM 2011*, pp. 1-5, 2011. [Article \(CrossRef Link\)](#)
- [3] B. M. Eldowek, S. M. A. El-Atty, and El-Rabaie, et al., "Second-Order Statistics Channel Model for 5G Millimeter-Wave Mobile Communications," *ARAB J SCI ENG*, vol. 43, no. 6, pp. 2833–2842, Jun. 2018. [Article \(CrossRef Link\)](#)
- [4] P. D. Diamantoulakis, K. N. Pappi, and G. K. Karagiannidis, et al., "Joint Downlink/Uplink Design for Wireless Powered Networks with Interference," *IEEE Access*, vol. 5, no. 99, pp. 1534–1547, Jan. 2017. [Article \(CrossRef Link\)](#)



- [5] Z. Wang, L. Ge, and T. Li, et al., “Energy efficiency maximization strategy for Sink node in SWIPT-enabled sensor-cloud based on optimal stopping rules,” *China Communications*, vol. 18, no. 1, pp. 222-236, Jan. 2021. [Article \(CrossRef Link\)](#)
- [6] X. Lu, P. Wang, and D. Niyato, et al., “Wireless Networks with RF Energy Harvesting: A Contemporary Survey,” *IEEE Commun. Surveys Tuts.*, vol. 17, no. 2, pp. 757–789, Nov. 2015. [Article \(CrossRef Link\)](#)
- [7] H. Tabassum, E. Hossain, and A. Ogundipe, et al., “Wireless-powered cellular networks: key challenges and solution techniques,” *IEEE Commun. Mag.*, vol. 53, no. 6, pp. 63–71, Jun. 2015. [Article \(CrossRef Link\)](#)
- [8] P. Vasant, J.A. Marmolejo, and I. Litvinchev, et al., “Nature-inspired meta-heuristics approaches for charging plug-in hybrid electric vehicle,” *WIREL NETW*, vol. 26, pp. 4753–4766, Oct. 2020. [Article \(CrossRef Link\)](#)
- [9] C. Psomas and I. Krikidis, “Energy Beamforming in Wireless Powered mmWave Sensor Networks,” *IEEE J. Sel. Areas Commun.*, vol. 37, no. 2, pp. 424-438, Feb. 2019. [Article \(CrossRef Link\)](#)
- [10] W. Chen, H. Ding, and S. Wang, et al., “Adaptive Discrete-Time-Switching-Based Energy-Harvesting Relaying Systems,” *IEEE Trans. Veh. Technol.*, vol. 68, no. 11, pp. 11064–11079, Sep. 2019. [Article \(CrossRef Link\)](#)
- [11] Y. Zeng and R. Zhang, “Full-duplex wireless-powered relay with self-energy recycling,” *IEEE Wireless Commun. Lett.*, vol. 4, no. 2, pp. 201–204, Jan. 2015. [Article \(CrossRef Link\)](#)
- [12] J. Guo, S. Zhang, and N. Zhao, et al., “Performance of SWIPT for full-duplex relay system with co-channel interference,” *IEEE Trans. Veh. Technol.*, vol. 69, no. 2, pp. 2311-2315, Feb. 2020. [Article \(CrossRef Link\)](#)
- [13] Y. Liu, Z. Wen, and N. C. Beaulieu, et al., “Power Allocation for SWIPT in Full-Duplex AF Relay Interference Channels Using Game Theory,” *IEEE Commun. Lett.*, vol. 24, no. 3, pp. 608-611, Mar. 2020. [Article \(CrossRef Link\)](#)
- [14] N. Garg, A. Rudraksh, and G. Sharma, et al., “Improved Rate-Energy Trade-Off for SWIPT Using Chordal Distance Decomposition in Interference Alignment Networks,” *IEEE Transactions on Green Communications and Networking*, vol. 6, no. 2, pp. 917-929, Jun. 2022. [Article \(CrossRef Link\)](#)
- [15] H. Ding, X. Wang, and D. B. D. Costa, “Adaptive Time-Switching Based Energy Harvesting Relaying Protocols,” *IEEE Trans. Commun.*, vol. 65 no. 7, pp. 2821–2837, Apr. 2017. [Article \(CrossRef Link\)](#)
- [16] A. A. Nasir, X. Zhou, and S. Durrani, “Wireless Energy Harvesting and Information Relaying: Adaptive Time-Switching Protocols and Throughput Analysis,” *IEEE TCOMMUN*, vol. 63, pp. 1607–1622, Mar. 2015. [Article \(CrossRef Link\)](#)
- [17] T. M. Hoang, A. El Shafie, and D. B. da Costa, et al., “Security and Energy Harvesting for MIMO-OFDM Networks,” *IEEE Trans. Commun.*, vol. 68, no. 4, pp. 2593-2606, Apr. 2020. [Article \(CrossRef Link\)](#)
- [18] N. Zhao, S. Zhang, F. R. and Yu, Y. Chen, “Exploiting Interference for Energy Harvesting: A Survey, Research Issues and Challenges,” *IEEE Access*, vol. 5, pp. 10403–10421, May. 2017. [Article \(CrossRef Link\)](#)
- [19] N. Lee and R. W. Heath Jr, “Advanced interference management technique: potentials and limitations,” *IEEE Wireless Commun.*, vol. 23, no. 3, pp. 30–38, Jun. 2016. [Article \(CrossRef Link\)](#)
- [20] J. Kakar and A. Sezgin, “A Survey on Robust Interference Management in Wireless Networks,” *Entropy*, vol. 19, no. 7, pp. 362, Jul. 2017. [Article \(CrossRef Link\)](#)
- [21] N. K. Breesam, W. A. Al-Hussaibi, and F. H. Ali et al., “Efficient Resource Allocation for Wireless-Powered MIMO-NOMA Communications,” *IEEE Access*, vol. 10, pp. 130302-130313, Dec. 2022. [Article \(CrossRef Link\)](#)
- [22] H. An and H. Park, “Energy-Balancing Resource Allocation for Wireless Cooperative IoT Networks With SWIPT,” *IEEE Internet Things J.*, vol. 9, no. 14, pp. 12258-12271, Jul. 2022. [Article \(CrossRef Link\)](#)

- [23] S. Bayat, A. Khalili and Z. Han, "Resource Allocation for MC MISO-NOMA SWIPT-Enabled HetNets with Non-Linear Energy Harvesting," *IEEE Access*, vol. 8, pp. 192270-192281, Oct. 2020. [Article \(CrossRef Link\)](#)
- [24] X. Gao, D. Niyato, and P. Wang, et al., "Contract Design for Time Resource Assignment and Pricing in Backscatter-Assisted RF-Powered Networks," *IEEE Wireless Commun. Lett.*, vol. 9, no. 1, pp. 42-46, Jan. 2020. [Article \(CrossRef Link\)](#)
- [25] S. Muy, D. Ron and J. R. Lee, "Energy Efficiency Optimization for SWIPT-Based D2D-Underlaid Cellular Networks Using Multiagent Deep Reinforcement Learning," *IEEE Syst. J.*, vol. 16, no. 2, pp. 3130-3138, Jun. 2022. [Article \(CrossRef Link\)](#)
- [26] Y. Xu, H. Xie, and C. Liang et al., "Robust Secure Energy-Efficiency Optimization in SWIPT-Aided Heterogeneous Networks with a Nonlinear Energy-Harvesting Model," *IEEE Syst. J.*, vol. 8, no. 19, pp. 14908-14919, Oct. 2021. [Article \(CrossRef Link\)](#)
- [27] L. Chen, B. Hu, G. Xu and S. Chen, "Energy-Efficient Power Allocation and Splitting for mmWave Beamspace MIMO-NOMA With SWIPT," *IEEE Sensors J.*, vol. 21, no. 14, pp. 16381-16394, Jul. 2021. [Article \(CrossRef Link\)](#)
- [28] S. A. A. Kazmi and S. Coleri, "Optimization of Full-Duplex Relaying System with Non-Linear Energy Harvester," *IEEE Access*, vol. 8, pp. 201566-201576, Oct. 2020. [Article \(CrossRef Link\)](#)
- [29] X. Peng, P. Wu, and H. Tan, et al., "Optimization for IRS-Assisted MIMO-OFDM SWIPT System with Nonlinear EH Model," *IEEE Internet Things J.*, vol. 9, no. 24, pp. 25253-25268, Dec. 2022. [Article \(CrossRef Link\)](#)
- [30] A. A. Nasir, X. Zhou, and S. Durrani, et al., "Relaying Protocols for Wireless Energy Harvesting and Information Processing," *IEEE Trans. Wireless Commun.*, vol. 12, no. 7, pp. 3622–3636, Jul. 2013. [Article \(CrossRef Link\)](#)
- [31] J. L, K. Z, and X. L, et al., "Research on Interference Energy Harvesting Based on SWIPT Relay System," in *Proc. of International Wireless Internet Conference*, pp. 430–439, May. 2018. [Article \(CrossRef Link\)](#)



**Jianxiong Li** received the B.S. and M.S. degrees in Physics in 1991 and 1994, respectively, and the Ph.D. degree in Communication and Information System in 2007, from Tianjin University, Tianjin, China. He is currently a Professor in School of Electronics and Information Engineering Tiangong, University, Tianjin, China. He is also with Tianjin Key Laboratory of Optoelectronic Detection Technology and Systems, Tianjin, China. His main research interests are in wireless power transfer, microwave technology and antenna, computational electromagnetics.



**Hailong Jiang** received the B.S. degree in Electronic Information Engineering from Yanshan University, Qinhuangdao, China, in 2018, where he is currently pursuing the M.S. degree with the School of Electronics and Information Engineering, Tiangong University, Tianjin, China. His current research interests include the simultaneous wireless information and power transfer.